Calculating the structure of spaceborne-lidar returns from the upper-level clouds

M.M. Krekova

Institute of Atmospheric Optics,
Siberian Branch of the Russian Academy of Sciences, Tomsk
Received December 18, 1998

Some results on return signals of a spaceborne lidar when used in sounding of the top level clouds and two-level cloudiness at $\lambda = 532$ nm have been calculated by Monte Carlo method. The estimates have been obtained for geometrical conditions corresponding to the parameters of BALKAN and LITE lidars. Some peculiarities in the signal formation and in the formation of the multiple scattering background are studied depending on the optical and geometrical conditions considered in the numerical experiments conducted.

This paper is a continuation of the cycle of papers devoted to the study of peculiarities in the formation of signals of a spaceborne lidar when sounding the clouds of different shapes and stratification. In Refs. 1–4 one can find estimates of the signals and analysis of structure observed in the water-droplet cumulus and stratus clouds of the lower level. The calculated results on return signals of a spaceborne lidar presented below refer to the upper level clouds.

Among the upper-level clouds there are cirrus clouds composed of ice crystal particles. These clouds may have different shapes, stratification, temperature regime, as well as different microstructure of the ensembles and dominating crystal habits.[5] Cirrus are the less studied object in aerology. Careful observation of cirrus is very important, because various physical and dynamic processes of cloud formation occur in the upper troposphere[6] (convection, turbulence, wave motion, etc.). In this connection, the interest of different specialists have appeared, especially in the last decade, in the study of optical properties, temperature, and dynamics of the upper-level clouds. Stratification of cirrus make it difficult to study those systematically, for example by means of a ground-based lidar instrumentation because of the presence of under-cloud aerosol layers, which can be relatively dense, or because of the presence of clouds in the lower layers of the atmosphere.

The *Ns-As-Cs* continuous cloud system often appears at the presence of active fronts. In this case the systematic observations of clouds with ground-based and airborne instruments become especially problematic. Taking this into account, one can see that optical measurements by means of a spaceborne lidar instrumentation seem to be quite promising, and the results presented in Refs. 7 and 8 are a good evidence of that.

The possible scope of problems that may be solved using spaceborne lidar systems can be determined from a model numerical experiment. The structure of a return signal from clouds was calculated by the Monte Carlo method under the boundary conditions that correspond to operation conditions of a spaceborne BALKAN lidar.[9] The main principles used in constructing of the algorithm have been described in Ref. 10.

It was supposed that a monostatic laser radar is being operated from the orbit at 400 km above the Earth surface. Its source of radiation isotropically emits a temporal delta-pulse within the cone of divergence angle $\varphi_i = 0.22$ mrad. The signal is recorded with a detector within a set of receiving field-of-view angles φ_d from 0.22 to 1.7 mrad. Optical properties of the scattering medium are presented by the extinction coefficient $\sigma_{ext}(z)$, the single scattering albedo $\Lambda(z)$, and the scattering phase function $g(\vartheta)$, where ϑ is the scattering angle. The aerosol extinction of radiation by the 30-km height atmospheric layer was taken into account in calculations. The vertical profiles $\sigma_{ext}(z)$ and $\Lambda(z)$ of atmospheric aerosol were determined according to the technique described in Ref. 11. The choice of optical characteristics of cirrus was based on the data available from literature.

According to Refs. 5 and 6, the mean value of the extinction coefficient for cirrus clouds of different types is $\sigma_{ext} \approx 2.5$ km^{-1}, and their geometrical thickness can reach 1.5 to 4 km. The altitude of their lower boundary over the ground surface is in the range from 6 to 13 km depending on latitude. It was supposed in calculating that the lower boundary of the upper-level clouds is within this range at the altitude of 8.5 km, and their thickness is $\Delta z = 1.5$ km. The results calculated in Ref. 12 were used to set the scattering phase function. The calculations have been performed using the geometric optics approximation for a polydispersion of hexagonal crystals assuming their random orientation in space. Authors of Ref. 12 have taken into account the particle size distribution characteristic of *Ci* and *Cs* clouds according to Ref. 13. The results are presented in the table and are convenient for using them as the initial data.

The structure of a lidar return taking into account the distribution of the multiplicity of interaction has been calculated by the Monte Carlo

0235-6880/99/04 362-06 $02.00

method with the statistics of 10 million photon paths for the optical thickness of a cloud layer $\tau \geq 2.5$. The number of photon paths has been proportionally increased as the optical thickness decreased. It is necessary for keeping the variance of the calculated functionals, which will be introduced below, within the limits of 10–15% at the end of a sounding path. The functionals are shown in Figs. 1–5 as functions of the parameter h that is equivalent to the photon path length in the scattering medium and is compared with the sounded layer position relative to the upper boundary of a cloud. The principal part of the results is presented for the field of view angle of $\varphi_d = 0.22$ mrad.

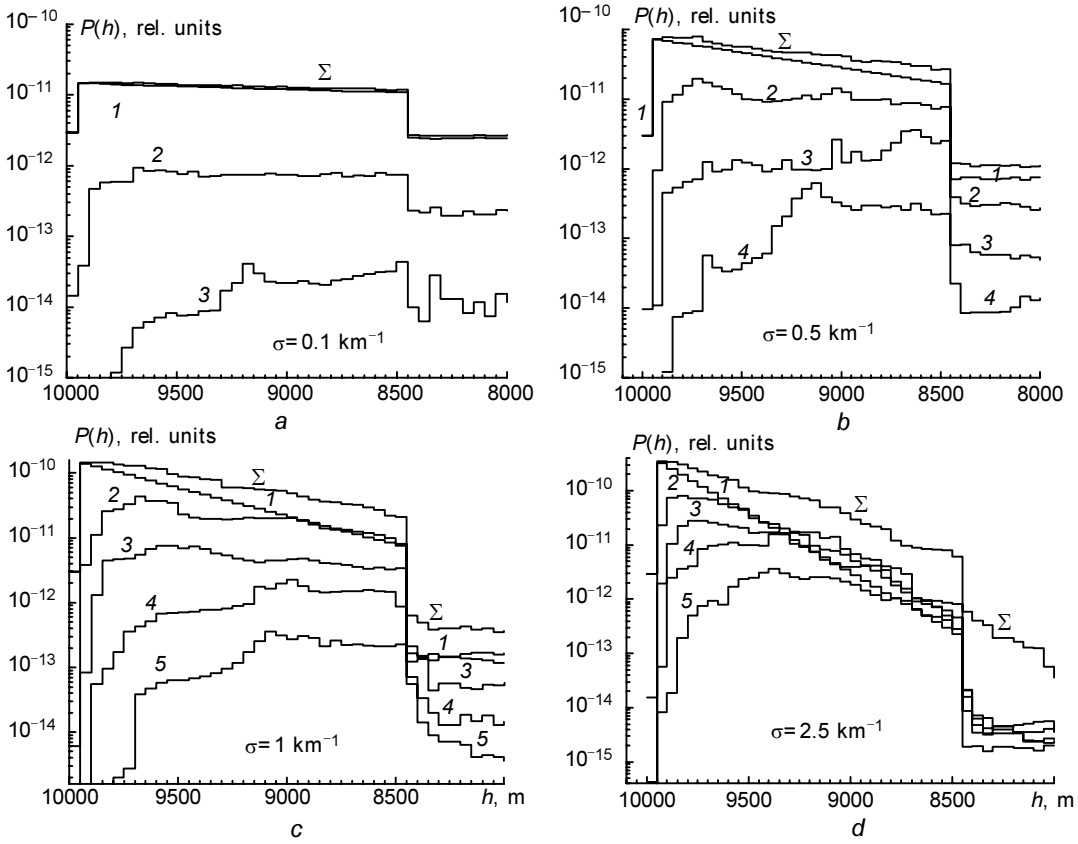

Fig. 1. The signal power $P(h)$ as a function of the penetration depth into the cloud and of the optical density of the medium. The numbers *1–5* at the curves correspond to the orders of multiplicity of scattering, the sign Σ corresponds to the total return signal.

Figure 1 shows some calculated results on the lidar signal power $P(h)$ due to different orders of multiple scattering for the clouds of different optical density that changes from 0.1 to 2.5 km^{-1}. The numbers at the curves correspond to the orders of multiple scattering and the sign Σ designates the power $P(h)$ of the total signal coming to the detector. The power signals is $P^{(K>1)} \ll P^{(1)}(h)$ for the medium with the optical density $\sigma_{ext} \leq 0.5$ km^{-1}, i.e. the total signal $P(h)$ is formed practically due to singly scattered radiation through the entire sounding path (see Figs. 1*a* and *b*). The results presented in Figs. 1*a, b,* and *c* show that the power $P^{(K>2)} \ll P^{(1)}(h)$ and the signal $P(h)$ from the sounding path with the $0.5 \leq \sigma_{ext} \leq 1$ km^{-1} is practically completely determined by two first orders of scattering. For the media having higher optical density, $\sigma_{ext} \approx 2.5$ km^{-1}, it is necessary to take into account the higher orders of multiple scattering. To satisfactorily describe the return signal at $\sigma_{ext} \approx 2.5$ km^{-1} (Fig. 1*d*) it is necessary to take into account five orders of scattering. One should note that the moment of a sharp decrease in the signal coincides with the lower boundary of the cloud layer, i.e. the qualitative behavior of $P(h)$ makes it possible to determine the cloud geometrical thickness quite exactly, within the limits of the time interval being gated. The results presented in Fig. 2 illustrate the change in the relative contribution from multiple scattering background $k(h) = P_b(h)/P(h)$ to the return signal along the sounding path for the clouds of different optical density. The level of the background contribution to the return signal $P(h)$ at the end of a sounding path is ~ 5% at $\sigma_{ext} \approx 0.1$ km^{-1} and increases up to 90% and more at $\sigma_{ext} \approx 2.5$ km^{-1}. That quick accumulation of the background component in the signal is provided not only by increased scattering volumes within the directional cone, but also by the strongly forward-peaked scattering phase function of particles in crystal

clouds.[12] The latter circumstance favors the fact that the radiation of high orders of multiple scattering does not leave the narrow directional cone up to significant optical depths. The dependence of the signal power $P(h)$ on the angular size of the receiver's field of view is shown in Fig. 3 for relatively transparent clouds, $\sigma_{ext} \approx 0.5$ km^{-1}, and for the visible ones with $\sigma_{ext} \approx 2.5$ km^{-1}. As the receiver's field of view angle increases, the absolute value of return signal increases along the entire sounding path due to multiply scattered radiation. The results show that the widening of the field of view angle φ_d up to approximately 1 mrad leads to the loss of possibility of determining the geometrical thickness of a cloud layer sounded, if its optical thickness exceeds $\tau = 2.5$. It follows from calculations shown in Fig. 3*a* that for the transparent clouds the above mentioned boundary of the receiver field of view angle is significantly wider and reaches 5 mrad, but it becomes proportionally more narrow as the geometrical thickness of clouds increases.

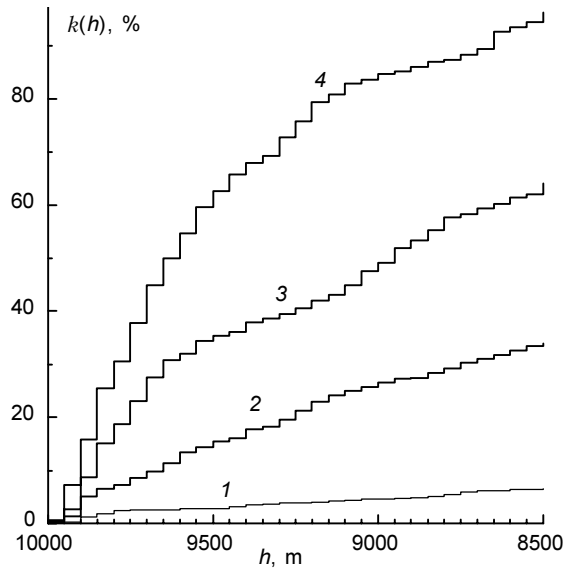

Fig. 2. The fraction of multiple scattering background $k(h)$ in the lidar return as a function of the depth into the cloud sounded and of its optical density. The curves *1–4* correspond to $\sigma = 0.1$, 0.5, 1, and 2.5 km^{-1}.

The calculations performed for cirrus of optically inhomogeneous vertical structure are shown in Fig. 4. The dependence $\sigma_{ext}(h)$ has been selected according to the data[6] on water content distribution in clouds. The qualitative behavior of the signals $P(h)$ in all three cases exhibits an inhomogeneous structure of the cloud, but signal maxima are diffuse. This occurs because the position of signal maximum due to single scattering, $P^{(1)}(h)$, which lays in the range $\tau \approx 0.5$–0.7, does not coincide with the position of maximum of the profile $\sigma_{ext}(h)$. Moreover, the maxima of $P^{(k)}(h)$ from the higher orders of multiple scattering are displaced toward larger values of the optical thickness. Figure 4*a* presents results calculated for a cloud, the total optical thickness of which $\tau_\Sigma \approx 1.7$, and the highest value of the extinction coefficient $\sigma_{ext}^{max}(h)$ is near $\tau \approx 1.05$, in the vicinity of which the signals of 2–4 orders of scattering gradually reach their maximum levels. As a result, the maximum of the signal $P(h)$ is only weakly pronounced and diffuse though it coincides with the position of $\sigma_{ext}^{max}(h)$.

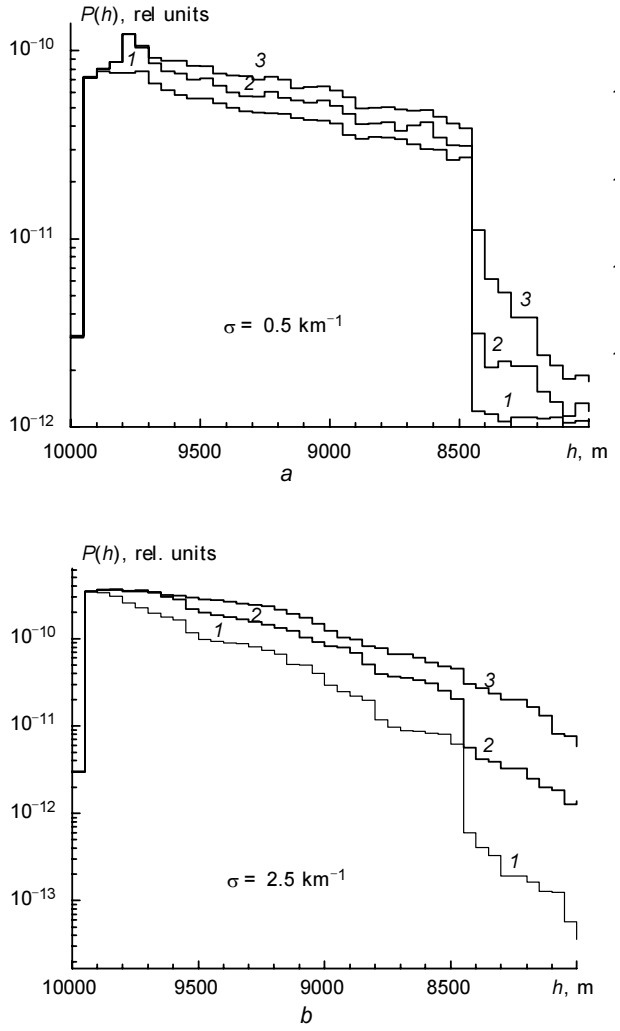

Fig. 3. The signal $P(h)$ as a function of the receiver's field of view angle φ_d calculated for the clouds with $\sigma_{ext} = 0.5$ (*a*) and 2.5 km^{-1} (*b*). Curves *1*, *2*, and *3* correspond to the field of view angles $\varphi_d = 0.22$, 0.88, and 1.7 mrad, respectively.

The results calculated for a cloud with $\tau_\Sigma \approx 2.2$ are shown in Fig. 4*b*. The value $\sigma_{ext}^{max}(h)$ occurs at the depth $\tau_\Sigma \approx 1.3$. In this case the maximum of the signal $P(h)$ is not only diffuse but it is displaced with respect to $\sigma_{ext}^{max}(h)$ toward a lower optical depth. Hence, the qualitative shape of a signal reflected from a cloud of an inhomogeneous vertical optical structure depends not only on the shape of the extinction coefficient profile but also on the peculiar features in formation of signals due to lower orders of scattering. It is

confirmed by the results calculated for the profile $\sigma_{ext}(h)$ having many maxima (Fig. 4*c*). In this example $\tau_\Sigma \approx 2$, the first maximum of the extinction coefficient profile is at the depth $\tau_\Sigma \approx 0.45$, the second maximum of $\sigma_{ext}(h)$ is at the same optical depth relative to the minimum. In this optical situation the extrema of the functions $\sigma_{ext}(h)$ and $P(h)$ practically coincide. The calculations show that a two or three-fold increase in the receiver's field of view angle relative to a preset one leads to violation of the agreement between the qualitative behavior of the above considered parameters. This is related to the increased fraction of higher orders of multiple scattering in the total return signal.

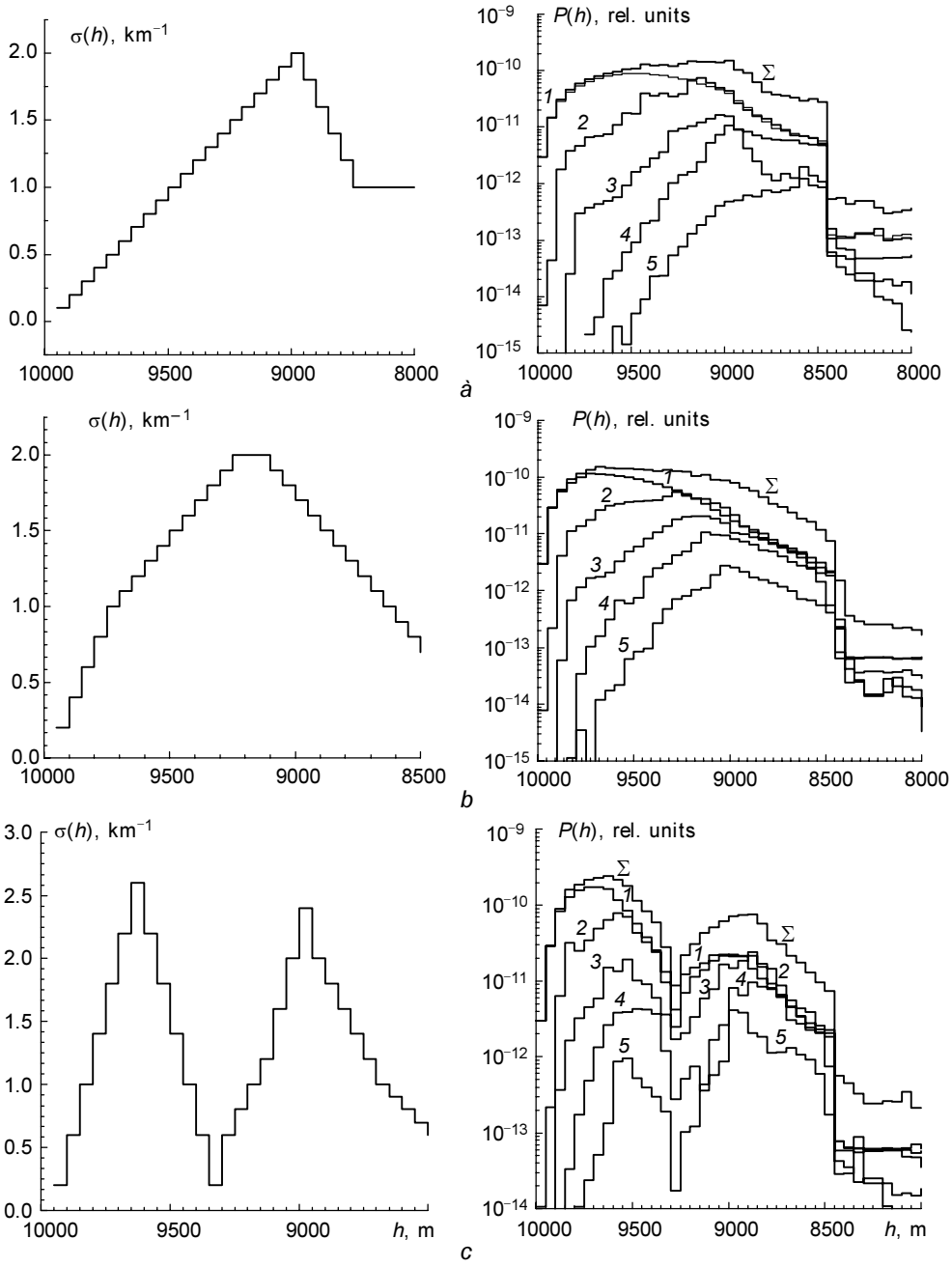

Fig. 4. The signal $P(h)$ calculated for the clouds of an optically inhomogeneous structure. The corresponding profiles of the extinction coefficient $\sigma_{ext}(h)$ are shown in the left-hand side panels, and the dependences $P(h)$ calculated with the separation of contributions coming from different orders of multiple scattering are shown in the right-hand side panels.

The next series of calculated estimates has been performed for the LITE lidar parameters and two-layer cloudiness. The appropriateness of the model experiment has been caused by the availability of a significant array of data obtained with this lidar,[14,15] as well as of the data of synchronous measurements with an airborne lidar. In some cases the geometrical thickness of clouds recorded with the spaceborne lidar

is significantly larger than the value measured with the airborne lidar. It is supposed that one of the causes of the signal broadening could be high level of the background due to multiple scattering. When inverting some experimental data, the optical depth of clouds measured with the airborne lidar sometimes exceeded that obtained with the spaceborne lidar, though, ideally, the situation observed should be the opposite. It follows from the fact that the scattering volume within the viewing cone of the spaceborne lidar and, hence, the background component of the signal is significantly larger than that for the airborne lidar. Numerical experiment is a necessary component in developing techniques for inverting the measurement data obtained.

It was supposed, as the initial data for the calculations, that the lidar is at the height $H = 250$ km above the Earth surface, the angle of the sounding beam divergence $\varphi_s = 0.6$ mrad, and the receiver's field of view angle $\varphi_d = 1.1$ mrad. It was assumed that there is a cirrus cloud (*Ci*) in the upper level at the altitude $h_1 = 10$ km, and its geometrical thickness is $\Delta h = 1.5$ km. A water-droplet cloud of the stratus type (*St*) having the thickness $\Delta h = 0.2$ km is assumed to be in the lower layer at the altitude of $h_2 = 2$ km. Its scattering properties correspond to the *C1* type of the classification from Ref. 16.

The calculated results on the return signal $P(h)$ from two-layer clouds with the extinction coefficients $\sigma_{ext} = 1.5$ km^{-1} for *Ci* and $\sigma_{ext} = 1.5$ km^{-1} for *St* are shown in Fig. 5*a*. The maxima of signals coming from the upper boundaries of clouds are within one order of magnitude. The calculations show that the signal coming from the low-level clouds is formed principally due to the radiation multiply scattered by the upper-level clouds if the optical density of the latter exceeds $\tau \approx 1$.

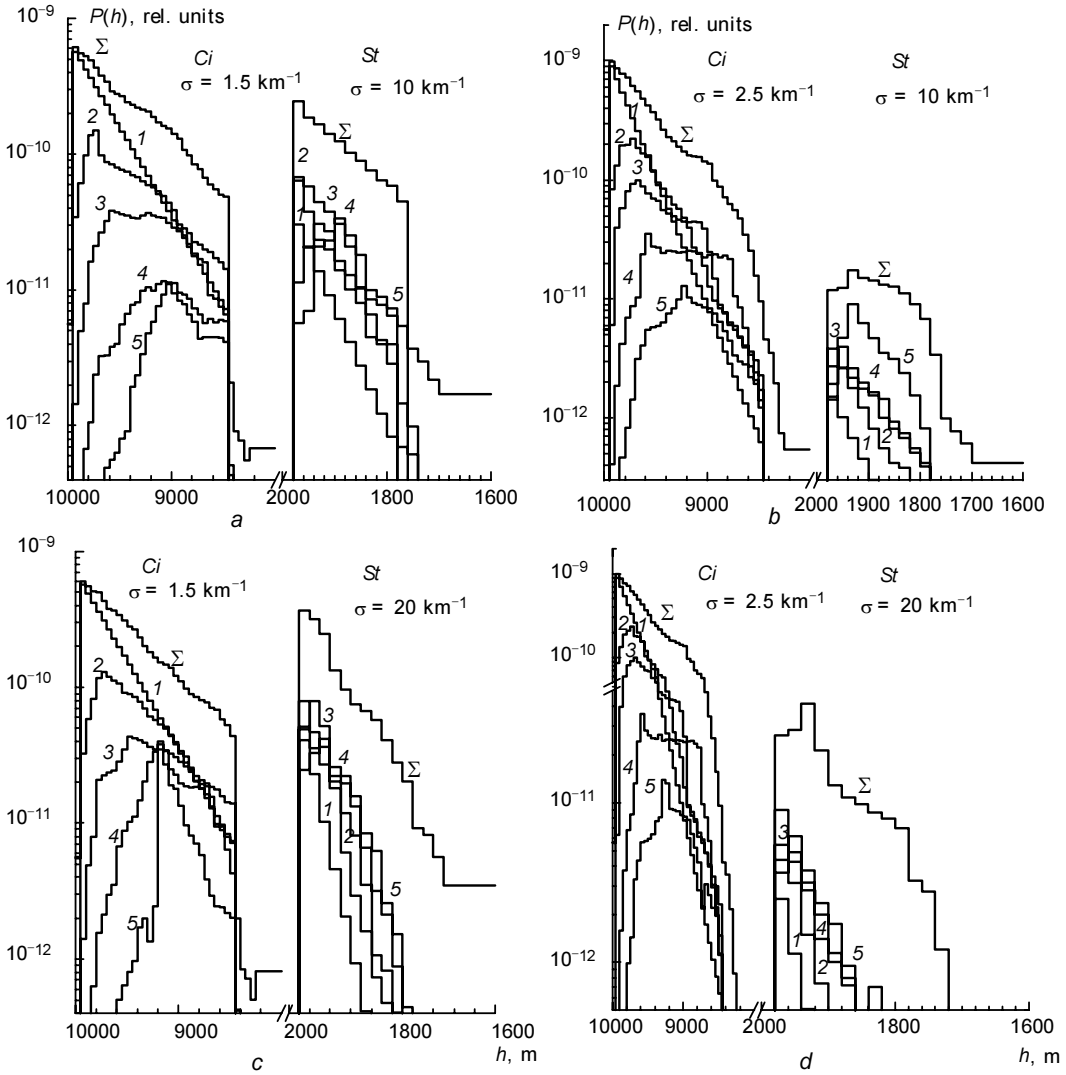

Fig. 5. Sounding of a two-layer cloudiness. The return signal $P(h)$ calculated with separation of the multiple scattering orders is shown for various optical densities of the upper- and low-level clouds.

The contribution coming from single scattering to the total return signal from *St* increases at lower values of τ of *Ci*. The sharp fall off observed in the pulse response from *St* occurs at the altitudes that are 40–60 m higher than its actual lower boundary. This is followed by more smooth variation of $P(h)$ with the height. One should note that the flux of radiation scattered by clouds is imposed on the return signal from the under-cloud aerosol layer having several hundred meters extension.

The increase in the optical density of the upper-level cloud up to $\sigma_{ext} = 2.5\ km^{-1}$ leads to a sharp decrease in the return signal $P(h)$ (Fig. 5*b*) from the low-level cloud. Besides, its temporal structure changes. In this case quite a sharp decrease in the trailing edge of the return pulse from *St* is biased relative to its lower boundary by 80–100 m. Obviously, the geometrical thickness of the low-level cloud can be determined accurate to this value. The confidence interval (20 m in this case) is related to the duration of the gating interval. Analogous calculations have been performed for the case of a higher optical density of the low-level cloud, the value of its extinction coefficient being $\sigma_{ext} = 20\ km^{-1}$. The calculated results are shown in Figs. 5*c* and *d*.

Some increase is observed in the absolute value of the return signal from the optically more dense medium of *St*. The qualitative behavior of the signal $P(h)$ from the low-level clouds shown in Fig. 5*c* agrees well with the behavior of the signal shown in Fig. 5*b*. Obviously, the reason for this is that the values of the total optical thickness of the two cloud layers ($\tau_\Sigma \approx 5.75$ in Fig. 5*b* and $\tau_\Sigma \approx 5.75$ in Fig. 5*c*) in both of these cases are close. This is confirmed by the results shown in Fig. 5*d* where the calculation has been performed for $\tau_\Sigma \approx 7.75$. In this case the temporal spread of the pulse $P(h)$ from *St* increases. The relatively sharp decrease of the trailing edge of the pulse is biased toward 120–140-m distance from the lower boundary of the cloud. Figure 5*c* shows the formation of a return signal from the low-level clouds. The contribution to the signal $P(h)$ increases as the order of multiple scattering increases. Therefore, extraction of information about the optical properties of the low-level clouds should use the techniques that consider the background component as a useful component of the signal.

Summarizing the above discussion, one can note the following: when sounding a two-layer cloudiness, extraction of information about the geometrical thickness of the low-level clouds with an acceptable accuracy is possible at $\tau_\Sigma \le 5$, while otherwise the absolute error increases from some tens to some hundred meters. Besides, the calculations performed for BALKAN and LITE lidars can be easily generalized to other lidars, given the geometrical size of the laser foot print on the upper boundary of the cloud layer is reduced to the same size. The absolute values of signals will differ depending on the position of a lidar with respect to the cloud layer sounded, but no large differences in the signal structure and its qualitative behavior should occur.

Acknowledgments

The work was supported in part by Russian Foundation for Basic Research (Grant No. 98–05–64066).

References

1. V.E. Zuev, G.M. Krekov, and M.M. Krekova, J. Appl. Optics. **26**, No. 15, 3018–3025 (1987).
2. M.M. Krekova and G.A. Titov, Opt. Atm. **1**, No. 9, 81–86 (1988).
3. G.M. Krekov and M.M. Krekova, Atmos. Oceanic Opt. **11**, No. 1, 42–45 (1998).
4. G.M. Krekov and M.M. Krekova, *ibid*, pp. 46–49.
5. I.P. Mazin and A.K. Khrgian, eds., *Clouds and Cloudy Atmosphere. Handbook* (Gidrometeoizdat, Leningrad, 1989), 648 pp.
6. A.K. Khrgian, ed., *Physics of Clouds* (Gidrometeoizdat, Leningrad, 1961), 460 pp.
7. D.M. Winkler and P.H. McCormick, Proc. Soc. Photo-Opt. Instrum. Eng. **2310**, 98–105 (1994).
8. J.D. Spinhirne and S. Palm, in: *Selected Papers of the 18th International Laser Radar Conference(ILRC)* (Springer Verlag ISBN 3-540-61887-2, Berlin,1996), pp. 213–216.
9. Yu.S. Balin, S.S. Samoilova, and A.A. Tikhomirov, Atmos. Oceanic Opt. **10**, No. 3, 209–220 (1997).
10. G.M. Krekov, M.M. Krekova, and V.S. Shamanaev, J. Appl. Optics **37**, No. 9, 1589–1595 (1998)
11. V.E. Zuev and G.M. Krekov, *Optical Models of the Atmosphere* (Gidrometeoizdat, Leningrad, 1986), 256 pp.
12. Y. Takano and K.-N. Liou, American Meteorological Society **46**, No. 1, 3–19 (1989).
13. A.J. Heumsfield and C.M.R. Platt, J. Atmos. Sci. **41**, 846–855 (1984).
14. W. Renger, C. Kiemle, H.-G. Schreiber, M. Wirth, and P. Moerl, in: *Final Results Workshop Proceedings* (Iroe-CNR, Florence, Italy, 1995), pp. 15–19.
15. J. Pelon, V. Trouillet, C. Flamant, P.H. Flamant, and R. Valentin, in: *Final Results Workshop Proceedings* (Iroe-CNR, Florence, Italy, 1995), pp. 31–36.
16. D. Deirmendjian, *Electromagnetic Waves Scattering on Spherical Polydispersions* (American Elsevier, New York, 1969).